Computational Research Progress in Applied Science & Engineering

ISSN 2423-4591

CRPASE Vol. 04, 19-26, Special Issue: The Second National & First International Conference on Soft Computing

Seismic Performance of Optimal Steel Moment Frames with Variation of Design Load Patterns

Mohsen Shahrouzi*, Ali Ojani

Engineering Department, Kharazmi University, Karaj, Iran

Keywords

Optimal seismic design,
Loading pattern,
Steel building frame,
Genetic algorithm,
Non-linear dynamic analysis.

Abstract

As a common practice, well-known building codes provide simplified design procedure based on equivalent lateral loading patterns, instead of performing rigorous dynamic step-by-step analyses. The present study concerns the effect of such lateral loading patterns on distribution of stiffness and strength in the structure and the resulted dynamic responses including failure sequence in the moment frames. Utilizing a genetic algorithm, design of the frame is fixed via sizing optimization under the corresponding equivalent static loads. Consequent structural responses for every such design are then derived via non-linear time-history analyses. Several issues are investigated in order to compare and rank the design patterns including minimal structural weight, sequence of plastic hinge formation and period shift due to non-linear seismic behavior. The results declare that the common code-based pattern is not necessarily the best in all the cases. Particularly, the proposed uniform-triangular distribution of base-shear can guide formation of plastic hinges to start from the less-critical stories in progressive collapse of moment frames.

1. Introduction

Due to the nature of earthquake excitations, the non-linear time history analysis (NLTHA) is perhaps the most accurate method for determining the seismic demand of structures. However, complexity and liability challenges have limited practical application of NLTHA. In the other hand, the equivalent static design procedure is popular and well-accepted by the seismic design codes due to its simplicity with respect to designs via spectral analysis or NLTHA. The choice of equivalent lateral load pattern is critical in this procedure. Height-wise stiffness and strength variation in the structure which is itself controlled by such design patterns can affect the corresponding seismic responses. Structures with inappropriate distributions of strength and stiffness have performed poorly in recent earthquakes due to several observed failures [1]. For example, the soft-story effect has been reported in several collapsed structures with non-suitable distribution of strength or stiffness. Therefore, the key point in such a simplified procedure is how a certain amount of base-shear is distributed among the structural levels.

The issue has been concerned by a number of researchers during the recent decades. Karami-Mohammadi et al. [1] studied the effects of using design code patterns such as those by uniform building code (UBC-97) [2] and national earthquake hazard reduction program (NEHRP) [3], on height-wise distribution of drift and ductility demand in a number of different lateral resistant building systems. According to their study, the codified strength distribution patterns do not lead to uniform distribution of ductility and deformation in steel shear-buildings or concentric braced frames subjected to severe earthquakes. This may not even lead to the best seismic performance of the structure. Applying non-linear analysis to some reinforced concrete frames, Hosseini and Motamedi [4] reported that true distribution of the base-shear over the buildings' height is not exactly the same as that predicted by the employed design codes. Similar observation is revealed by Lee and Goel [5] analyzing 2 to 20 story frames subjected to various earthquake excitations. Chopra [6] tested several shear-buildings under El-Centro 1940 record taking the story yield-strength of these models in accordance with the load patterns of UBC-97 [2]. He concluded that such a distribution pattern does not lead to equal ductility demand in all stories and such a demand is higher for the first story in most of the treated cases. Moghaddam and Esmaeilzadeh-Hakimi [7] proposed special patterns of story yield-strength distribution for a number of shear building models. As a result, they achieved less ductility demand in uniform distributions with respect to those of UBC-97. Moghaddam and Hajirasouliha [8] utilized theory of uniform height-wise story deformation demands using the optimality criteria to find proper loading patterns

* Corresponding Author:
E-mail address: shahruzi@khu.ac.ir – Tel, (+98) 2634569555 – Fax, (+98) 2634569555

Received: 18 January 2018; Accepted: 12 March 2018

under different dynamic characteristics of the structure and the seismic excitation. Ganjavi et al. [9] treated a number of reinforced concrete buildings based on equivalent static loading procedure in ICSDB-05 (Iranian Code for Seismic Design of Buildings) [10] considering height-wise distribution of hysteretic energy, drift and damage subjected to four earthquake records. They observed relatively intense concentration of drift and damage in one or two stories of a building. Chao, et. al. [11] proposed a lateral load pattern based on statistical study of inelastic story-shear distribution. They observed that the newly designed frames under such a procedure experienced more uniform inter-story drifts with respect to the common code practice. Motamedi and Nateghi [12] proposed a triangular-rectangular pattern based on ICSDB-05. The results of inelastic time history analyses confirmed that seismic energy distribution along the height of buildings is more uniform by their proposed lateral load pattern than by the design codes. Shahrouzi and Rahemi [13] presented a simultaneous optimization of structural sizing and lateral loading pattern. Utilizing linear dynamic analyses, it was shown that their proposed optimal lateral load pattern led to better safety and more economic design than traditional code-based by avoiding stress concentration in more crucial stories.

The present study concerns effect of different lateral load patterns on the failure sequence of moment frames regarding their non-linear behavior. Afterwards, design of frame members is fixed via sizing optimization under each loading pattern. The well-known genetic algorithm is utilized for the peresent work among several other metaheristics [14-20]. Consequently, structural response for every such design is derived by NLTHA. A number of issues are investigated in order to compare and rank the design cases including optimal building's weight, variation of plastic hinge sequence and fundamental period-shift due to seismic excitation.

2. Lateral Design Load Patterns

Three *Loading Patterns*, LPs are introduced here-in-after for height-wise distribution of the codified base-shear, $V_{0,static}$. They are listed below as depicted in Figure 1

- LP (I): Base-shear distribution according to UBC-97 and ICSDB-05.This height-wise distribution of lateral forces is to be determined from Eq. (1)

$$F_i = \frac{w_i h_i}{\sum_{j=1}^{N} w_j h_j} \cdot (V_{0,static} - F_t) \tag{1}$$

where w_i and h_i are the weight and height of the ith floor above the base, respectively, N is the number of stories, $V_{0,static}$ is the codified base-shear and F_t is the additional force at the top floor to account for the higher modes' effect. For a fundamental period, T, greater than 0.7 s, the value of F_t in Eq. (1) is $0.07TV_{0,static}$, otherwise it is taken zero. This pattern forms the upper triangular shape when story masses are equal and F_t is zero.

LP (II): Rectangular shaped uniform distribution of base-shear along the height of building.

LP (III): Rectangular-triangular pattern including combined uniform distribution and triangular distribution at the uppermost one-third of the structure's height.

3. Optimization Problem Formulation

For each design of steel moment frame, a combination of member profiles is to be selected among available cross-sections. However, only a portion of such a member sizing design-space will be considered feasible/allowable according to the design code requirements [13].

Several possible designs may satisfy the feasibility conditions; however, leading to quite different seismic responses. In order to unify a design among them, an optimal set of frame sections which corresponds to minimal structural weight is determined satisfying AISC-ASD89 (Allowable Stress Design by American Institute of Steel Construction) [21] design regulations and the allowable story displacement/drift limitations due to ICSDB-05 [10]. The optimization problem is thus formulated as follows:

$$Minimize \quad W = \sum_{i=1}^{Number\,Of\,Members} \rho . A_i . L_i \tag{2}$$

subjected to

$$\left| \frac{\Delta^j}{\Delta^j_{all}} \right| - 1 \le 0, \; j = 1, \ldots, \text{Number of stories} \tag{3}$$

$$\left| \frac{SR_i}{SR_i^{all}} \right| - 1 \le 0 \tag{4}$$

$$\begin{aligned} &\text{if } T \le 0.7^s : \; \Delta^j_{all} = \frac{0.025 h_j}{0.7R}, \\ &\text{otherwise} : \Delta^j_{all} = \frac{0.020 h_j}{0.7R} \end{aligned} \tag{5}$$

$$\begin{aligned} &\text{if } \frac{f_a}{F_a} > 0.15 : SR = \frac{f_a}{F_y} + \frac{f_{bx}}{F_{bx}} + \frac{f_{by}}{F_{by}} \text{ , otherwise :} \\ &R = \max \left\{ \begin{array}{l} \dfrac{f_a}{F_a} + \dfrac{C_{mx} f_{bx}}{(1 - \frac{f_a}{F'_{ex}}) F_{bx}} + \dfrac{C_{my} f_{by}}{(1 - \frac{f_a}{F'_{ey}}) F_{by}} \\ \& \\ \dfrac{f_a}{0.60 F_y} + \dfrac{f_{bx}}{F_{bx}} + \dfrac{f_{by}}{F_{by}} \end{array} \right\} \end{aligned} \tag{6}$$

where W stands for the structural weight as the objective function, ρ is the material density, L_i and A_i denote length and cross-sectional area of the ith member, SR_i and SR_i^{all} denote the ith member combined stress-ratio and its allowable limit (unity) according to AISC-ASD89, respectively. f_a and f_b are the resultant axial and bending stresses while F_a and F_b denote the corresponding allowable axial and bending stresses, respectively. $F_e^{'}$ is the Euler stress divided by a safety factor due to AISC-ASD89. C_m is a codified coefficient representing distribution of moment along the member length for sway/moment frames taken as C_m=0.85. h_j stands for the jth story height while R denotes the behaviour factor due to ICSDB-05. Δ^j and Δ^j_{all} are the jth story drift and its allowable limit, respectively.

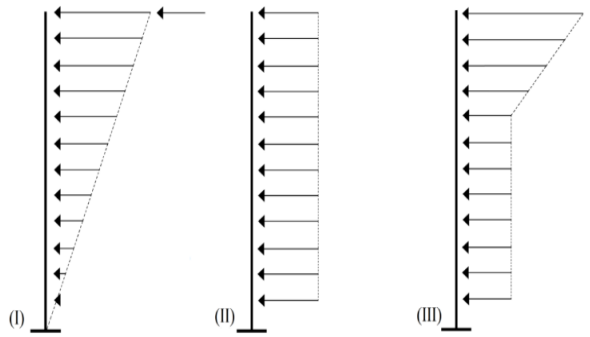

Figure 1. The employed lateral load patterns, (I) upper triangular, (II) uniform, (III) combined

The members in a structural model can be categorized into *N* distinct groups in order to deserve symmetry or other practical issues in the design. Any such group may be further assigned a section index from a discrete list of available sections. Thus, the design vector $\underline{X} = \{x_1, x_2, ..., x_N\}$ is defined so that any its component, x_i can be assigned an integer section number between x_i^{LB} and x_i^{UB}.

$$x_i^{LB} \le x_i \le x_i^{UB}, \quad i = 1, 2, ..., \text{Number of member groups} \tag{7}$$

Such a definition of design vector truly constructs the discrete sizing design space to be further searched by an optimization algorithm. It is most beneficial in cases (like the present problem) that more than one structural property (e.g., section area, moment of inertia and so on) is derived from every section ID. As soon as all components of such a design vector $\underline{X}$ are filled with section indices, it is decoded to a frame model to be further analysed in order to evaluate if it satisfies the design code constraints. The proposed optimization problem is well suited for meta-heuristic algorithms with capability of searching the discrete design spaces. One of common methods in such a category is the *Genetic Algorithm*, GA. Since its formal presentation by Holland [22], many GA variants have been successfully applied to engineer problems [14, 23].

The proposed definition of the design vector corresponds to a *direct index coded* GA [23]. It is employed here in order to efficiently search the design space avoiding challenges such as Hamming cliffs. Any value assigned to a gene is called its allele which is an integer number in the current direct encoded chromosome. Figure 2 shows a sample direct index crossover. Similarly direct index mutation is defined by substituting a current allele with another value in its corresponding list of indices [23].

Figure 2. Sample one-point direct-index crossover

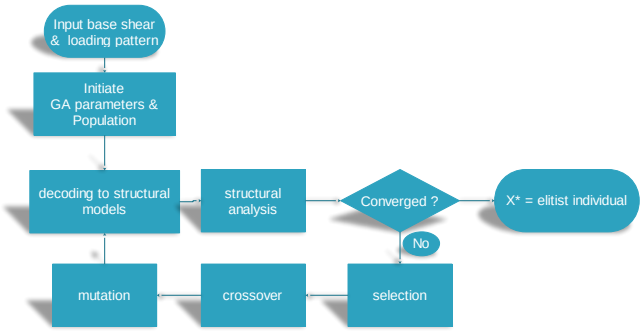

Figure 3. Flowchart of the utilized genetic algorithm

In the employed GA a population of chromosomes are first generated by randomly assigning any x_i, an index between x_i^{LB} and x_i^{UB}. Every chromosome is then decoded to a structural model and its fitness is evaluated using Eq. (8). Such a penalty approach takes into account both economy associated with W and safety constraints as:

$$Fitness(\underline{X}) = -W\left(1 + K_{P1}C_1 + K_{P2}C_2\right) \tag{8}$$

K_{P1} and K_{P2} are the penalty coefficients. C_1 is violation of the codified displacement constraint and C_2 is the combined stress-ratio constraint violation according to AISC-ASD89 and ICSDB-05.

Once all chromosomes in a generation are evaluated, the fittest ones are transferred to the next generation via *tournament selection*. Direct index mutation and one-point crossover are the other GA operators employed to generate the next population. Using an elitism strategy, the best chromosome of every previous population is substituted with the worst of the current in order not to lose the fittest during generations of the search. The algorithm iterates up to the last iteration as demonstrated in the flowchart of Figure 3. Finally, the elitist chromosome is decoded as the optimal design.

4. Numerical Simulation

Planar examples of low- and medium-rise steel buildings are studied here with given topologies and boundary conditions. For each model there may be several sets of sections which satisfy the design code regulations; however, leading to different dynamic responses. Therefore, a screening methodology is needed to unify the frame design prior to study its nonlinear behaviour. In this regard, the design of each example due to any of the three LP's is first fixed by sizing optimization under equivalent static loading. The well-trusted genetic algorithm is employed for such a design phase. Control paramaters of GA are tuned after a number of trials as given in Table 1. For such a sizing optimization problem, the penalty constants in the fitness function are taken 10 and 5 for K_{P1} and K_{P2}, respectively.

Table 1. Control parameters of the employed GA

$N_{Population}$	$P_{crossover}$	$P_{mutation}$	N_{Iters}
30	0.85	0.03	1000

It is worth notifying that for each example the static base-shear is taken identical but its height-wise distribution is changed by the exerted loading pattern to guide the arrangement of stiffness and strength in the frame.

4.1. Optimal Design under Various Loading Patterns

Two examples are studied with symmetric member grouping of Figure 4; i.e. 8-story and 15-story frames both with 2-bays. The story height is uniformly taken $3m$ while all bay lengths are fixed to $4m$. Material peroperties include rigidity modulous of $196\,GPa$ and yield stress of $235.4\,MPa$.

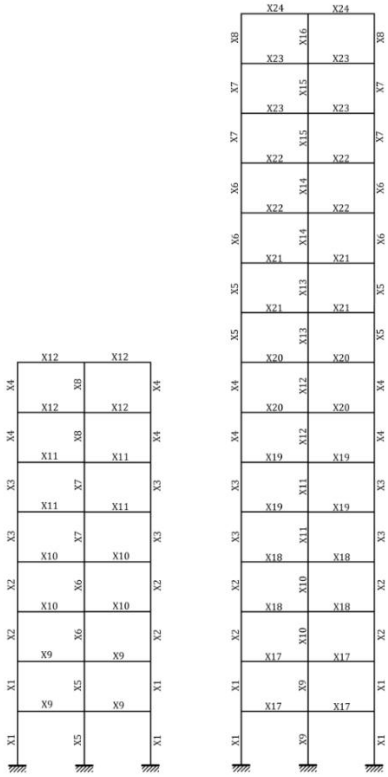

Figure 4. Boundary conditions and symmetric member grouping of the treated examples

Table 2. Available sections for optimal design of each example

ID	8-story	15-story
1	HE100B	HE200B
2	HE120B	HE220B
3	HE140B	HE240B
4	HE160B	HE260B
5	HE180B	HE280B
6	HE200B	HE300B
7	HE220B	HE320B
8	HE240B	HE340B
9	HE260B	HE360B
10	HE280B	HE400B
11	HE300B	HE450B
12	HE320B	HE500B
13	HE340B	
14	HE360B	
15	HE400B	

Table 2 gives the available sections for sizing optimization of each exmple. It is worth mentioning that cardinality of the design space for the 8-story frame is $15^{12} \approx 1.3\times10^{14}$ and it has the order of 10^{25} for the 15-story example. Therefore, enumeration of all such alternatives is not practical. Instead, GA is employed to capture optimal solution by sampling a fraction of such large design spaces.

The constraints are evaluated by static analysis under combined gravitational and lateral loadings due to the design code regulations; ICSDB-05 [10]. In this regard, the codified base-shear is calculated by equivalent static design procedure of ICSDB-05 and then distributed among height of the structure in accordance with the patterns (I), (II) or (III). Sizing of every example under each load pattern results in a distinct frame design; i.e. 3 designs for the first and 3 designs for the second example. Note that the static base-shear is taken identical for each of the two examples.

According to Table 3, in both examples the uniform pattern LP-(II) has led to the least optimal weight of the steel frame. The matter is better declared in convergence curves of Figures 5 and 6 for the 8-story and 15-story examples, respectively. These figures exhibit that the final design in each case has been announced after GA has converged with no further improvement. It can be concluded that the loading pattern of the current design code is less economic among the patterns of concern.

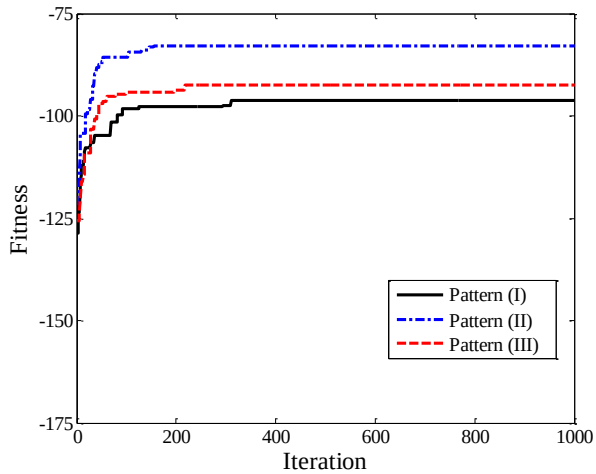

Figure 5. Convergence history of GA for various load patterns in the 8-story example

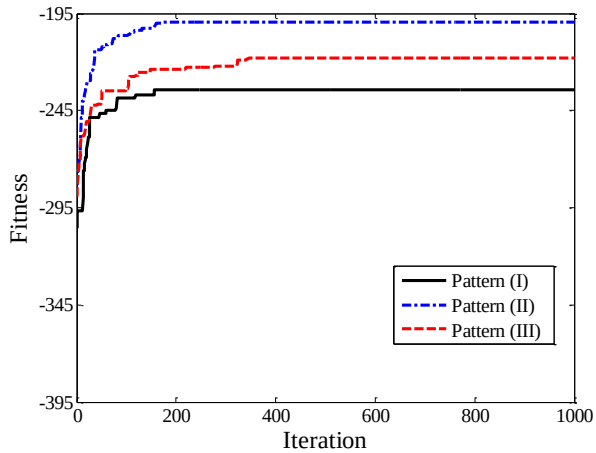

Figure 6. Convergence history of GA for various load patterns in the 15-story example

Table 3. Structural weight of optimal designs (kN)

Loading Pattern	(I)	(II)	(III)
8-story	95.5	83.5	92.0
15-story	231.8	197.2	216.2

4.2. Non-linear Behavior Detection via Dynamic Analyses

Once sizing of each example under any loading pattern led to a distinct frame design, its behaviour is studied by evaluating modal and nonlinear dynamic responses against a number of earthquakes. The selected input records are shown

in Figure 7. Table 4 reports characteristics of the employed ground motions as the source of seismic excitation in the analysis phase [24]. For the sake of fair comparison, any such record is scaled to the design spectra using soil type-III and very high seismicity province of ICSDB-05 [10].

Table 4. Applied Strong Ground Motions

Earthquake		Station	Magnitude	PGA/g
Kobe	1995	KJMA000	6.9	0.821
Northridge	1994	NWH090	6.7	0.583
Tabas	1978	Tabas-LN	7.4	0.836

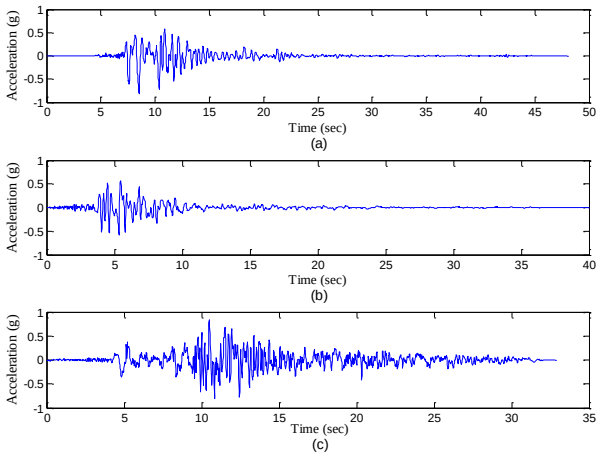

Figure 7. Time history plot of seismic accelerograms: (a) Kobe-1995, (b) Northridge-1994, (c) Tabas-1978

In the absence of experimental results, nonlinear properties of plastic hinges are determined here based on the FEMA356 recommended curves with a strain-hardening branch with 3% of the initial elastic stiffness [25]. In this regard, deformation-controlled nonlinear components are utilized; where combined axial-bending plastic-hinges are associated with the column ends and pure bending hinges are assigned to the flexural beams.

An important measure to compare non-linear behavior is the ratio of dynamic to static base-shear. It is called *peak normalized nonlinear base-shear;* denoted by α as:

$$\alpha = \frac{V_{0,Dyn-NL}}{V_{0,Static}} \tag{10}$$

$V_{0,Dyn-NL}$ is the maxium base-shear among time increments of the non-linear dynamic analysis. $V_{0,Static}$ is the design base shear determined due to static procedure of the seismic code of practice; ICSDB-05.

Table 5 reveals comparison of the resulting values of α . It is evident that in both examples, the most seismic demand belongs to pattern (I) while pattern (II) has experienced less base-shear from the same earthquake excitations when averaged over entire time of the input accelerogram record.

Table 5. Mean peak normalized base-shear among the treated seismic excitations

Loading Pattern	(I)	(II)	(III)
8-story	4.07	3.23	4.03
15-story	4.00	3.39	4.18

Effect of different design patterns on structural characteristics is further studied from an interesting view-point: gradual loss of structural redundancy as the plastic hinges arise more and more toward an unstable mechanism. Here, an equivalent period is defined for the frame at a certain stage of plastic hinge formation; i.e. the stage where the first plastic-hinge overpasses the immediate occupancy limit due to FEM356 regulations. An equivalent period at the start of plastic phase ; T_{ps} is determined suppressing any rotational stiffness at the location of plastic hinges that are first formed in the moment frame. Consequently, the normalized period shift from its initial value T_e in the elastic phase to such an equivalent plastic model of the structure is taken a measure of redundancy loss in the frame. It is determined by a period shift factor; β as:

$$\beta = 100 \times \frac{T_{ps} - T_e}{T_e} \tag{9}$$

According to Table 6, the design under LP-(II) has the greatest period shifts in the 8-story eample. It may be related to the lightest structural members in LP-(II) with respect to the other two designs. The least mean β in this example belongs to the LP-(III) design, however, it has been more sensitive to the applied earthquake excitations.

Table 6. Period shift percentage among various excitations and loading patterns in the 8-story example

		Loading Pattern		
Earthquake		(I)	(II)	(III)
Kobe	1995	1.1	2.0	0.5
Northridge	1994	1.1	2.0	0.5
Tabas	1978	1.1	2.0	1.8
average		1.1	2.0	0.9

Table 7. Period shift percentage among various excitations and loading patterns in the 15-story example

		Loading Pattern		
Earthquake		(I)	(II)	(III)
Kobe	1995	1.1	5.2	4.2
Northridge	1994	0.8	8.1	2.2
Tabas	1978	1.2	30.3	1.2
average		1.0	14.8	2.5

Table 7 gives β for the 15-story example. Higher amount of period shifts, again, belongs to the LP-(II) confirming its higher potential for redundancy loss under exerted earthquakes. Comparison of results in Tables 6 and 7 shows that the taller frame is more sensitive to the seismic excitation regarding β measure.

As another issue, variation of the plastic hinge formation sequence among the story columns is studied due to variation of the applied loading pattern. Nonlinear time-history analysis under given set of earthquakes is employed for this phase. Table 8 gives such a sequence for each LP by the numbers corresponding to the stories where column plastic hinges arises one after the other.

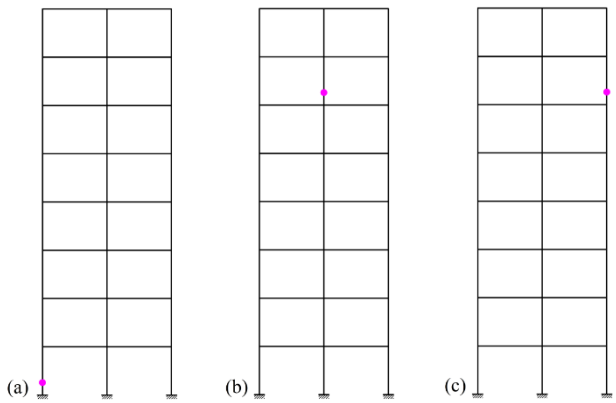

Figure 8. Location of pioneer plastic hinges under Kobe-1995 in optimal designs due to (a) LP-I, (b) LP-II , (c) LP-III

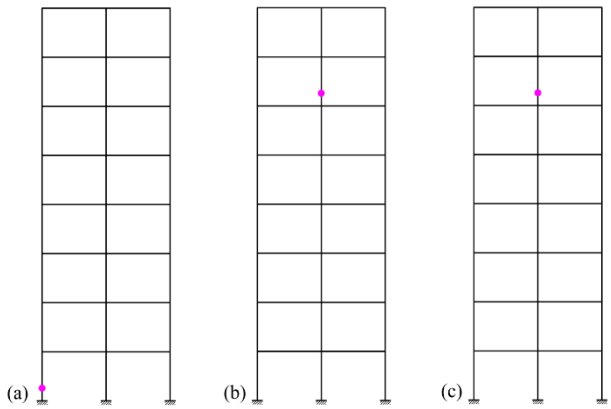

Figure 9. Location of pioneer plastic hinges under Northridge-1994 in optimal designs due to (a) LP-I, (b) LP-II , (c) LP-III

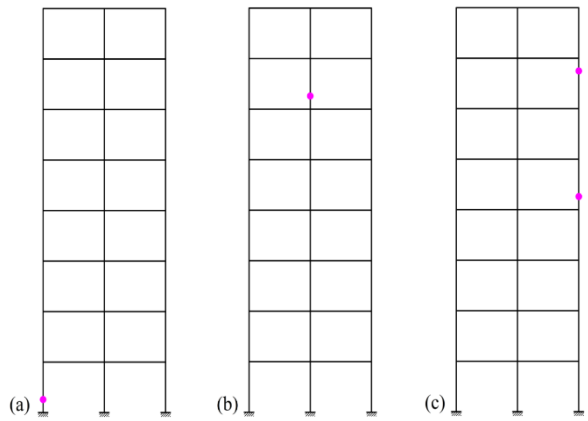

Figure 10. Location of pioneer plastic hinges under Tabas-1978 in optimal designs due to (a) LP-I, (b) LP-II , (c) LP-III

It can be noticed that applying LP-(I) in the design has led such plastic hinges to start at the first story. As columns at this lowest story undergo the most gravitational loads in combination with sway effects so they are distinguished the most critical ones for the overall structural stability. In contrary, patterns (II) and (III) have shown better performance leading formation of plastic-hinges to start from the 7th and the 5th stories, respectively. The matter is graphically declared in the Figure 8 for three applied patterns under the Kobe-1995 earthquake. Figure 9 shows similar results for Northridge-1994 excitation. According to Figure 10, formation of the 1st plastic hinge is slightly different under Tabas-1978 earthquake in the 3rd model which is designed to the LP-(III); that is simultaneous formation of two plastic hinges in the 5th and the 7th story columns.

Table 8. Sequence of plastic hinge formation in the 1st example

Earthquake	LP	Story sequence							
Kobe1995	(I)	**1**	2	5	7	6	3		
	(II)	7	5	**1**	3	4	6		
	(III)	7	3	5	8	6	**1**	4	2
Northridge1994	(I)	**1**	2	3	5				
	(II)	7	**5**						
	(III)	7	3	**1**	4	5			
Tabas 1978	(I)	**1**	5	3	2	7	6	4	
	(II)	7	5	6	3	**1**	4	2	
	(III)	7,5	**1**	3	4	2	8	6	

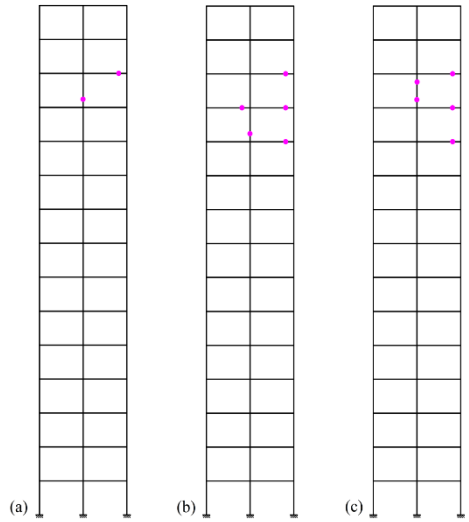

Figure 11. Location of pioneer plastic hinges under Kobe-1995 in optimal designs due to (a) LP-I, (b) LP-II , (c) LP-III

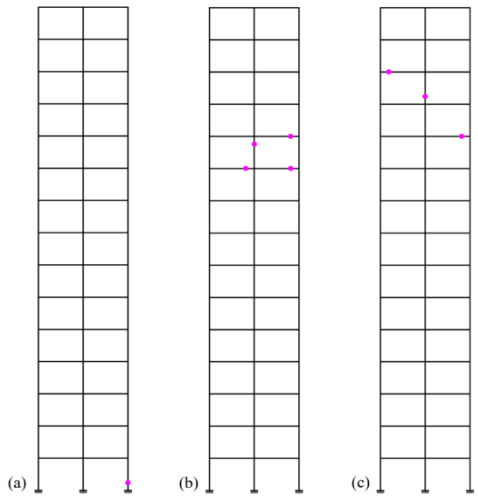

Figure 12. Location of pioneer plastic hinges under Northridge-1994 in optimal designs due to (a) LP-I, (b) LP-II , (c) LP-III

Sequence of plastic hinge formation for sizing designs under each LP in the 15-story example are shown in Figures 11, 12, 13 for the exctitation redords: Kobe-1995, Northridge-1994 and Tabas-1978, respectively. It is observed that only LP-(I) has made plastic hinge to start at the 1st story columns which is more dangerous for overall stability of the frame. LP-III, however, revealed better performance from this point of view. It can be also noticed

that LP-(II) can result in wider distribution of plastic hinges in such stages of entrance to nonlinear structural behavior.

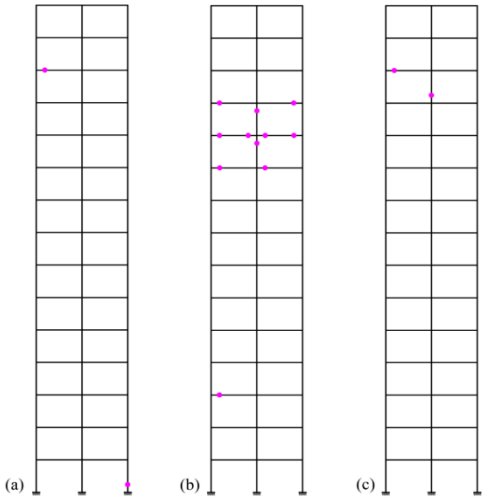

Figure 13. Location of pioneer plastic hinges under Tabas-1978 in optimal designs due to (a) LP-I, (b) LP-II , (c) LP-III

5. Summary and Conclusion

In the present work, the procedure of design and analysis was distinguished in two distinct phases; first screening several possible designs by means of sizing optimization and next studying the behaviour of uniquely revealed optimal designs via NLTHA as a more accurate dynamic analysis for building moment frames.

Three main lateral loading patterns were then studied due to their simplicity of advice to engineering community including upper-triangular, uniform and mixed patterns. Applying each pattern in the design phase, distribution of stiffness and strength among the frame members were guided according to each selected LP. As a result, the minimal structural weight found least for the uniform pattern LP-(II) and most for the codified upper-triangular one LP-(I), however, such differences was nearly less than 20% among treated loading patterns.

The optimally designed models were further treated by a number of seismic excitation records via NLTHA and the effect of design patterns are investigated via some interesting following issues, i.e.; design preference for structural stability, redundancy loss, and dynamic base-shear demand under exerted time-history excitations. In the light of the current study some remarks can then be concluded as

- Economical merit of the optimal design is directly affected by the selected pattern of distributing the same static-base shear among the frame height as equivalent lateral loads.

- The pattern LP-(I) can led sequence of plastic-hinge formation to start from lower story columns which are considered more critical in the structural stability. Therefore, other design patterns should be considered to reduce such potential of stability loss and consequent progressive collapse.

- Design pattern LP-(II) which uniformly distributes equivalent loads can dissipate seismic input energy via more plastic hinges in a wider region among the frame members.

- In all the examples and treated seismic records, the uniform pattern LP-(II) led to more period shift regarding its more economical structural weight.

- In both the examples, the design under LP-(II) experienced lower dynamic base-shear and required less demand to the force reduction factor during its entrance to the nonlinear phase.

According to the aforementioned results via the treated examples, LP-(III) which combines desired features of the uniform and upper-triangular patterns, is an interesting alternative to common practice. Investigating more behavioral aspects by applying wider range of ground motion records will, of course, be a future scope of work.

References

[1] R. Karami-Mohammadi, M.H. El Naggar, H. Moghaddam, Optimum Strength Distribution for Seismic Resistant Shear Building, Solids and Structures 41 (2004) 6597–6612.

[2] International Conference of Building Officials, Uniform Building Code (UBC-97) Whittier, CA, US, 1997.

[3] Building Seismic Safety Council, Recommended Provisions for Seismic Regulations for New Buildings and Other Structures, NEHRP, Washington, US, 1997.

[4] M. Hosseini, M. Motamedi, A study on the distribution of lateral seismic forces in the height of R/C buildings by using nonlinear dynamic analysis, 1st Conference of Iranian Society of Civil Engineers (ISCE), Tehran, Iran, (1999). (In Persian)

[5] S.S. Lee, S.C. Goel, Performance based seismic design of structures using target drift and yield mechanism, In: US Japan Seminar on Advanced Stability and Seismicity Concept for Performance Based Design of Steel and Composite Structures Kyoto, Japan, (2001).

[6] A.K. Chopra, Dynamics of structures: theory and applications to earthquake engineering, 2nd Ed., Prentice Hall Inc, London, 2001.

[7] H. Moghaddam, B. Esmaeilzadeh-Hakimi, On the Optimum Seismic Loading of Multistory of Structures, 3rd International Conference on Seismology and Earthquake Engineering, Tehran (1999) 669–676.

[8] H. Moghaddam, I. Hajirasouliha, A new approach for optimum design of structures under dynamic excitation, Asian Journal of Civil Engineering 5 (2004) 69–84.

[9] B. Ganjavi, J. Vaseghi-Amiri, G. Ghodrati-Amiri, A.R. Sarvghad-Moghaddam, Distribution of damage, absorption and loss of seismic energy in moment resisting RC frames (MDOF). 2nd National Congress on Civil Engineering, Tehran, Iran, (2005). (In Persian)

[10] Building and Housing Research Center, Iranian Code for Seismic Resistant Design of Buildings Standard No. 2800-05. 3rd Ed., Tehran, Iran, 2005.

[11] S.H. Chao, S.C. Goel, S.S. Lee, A Seismic Design Lateral Force Distribution Based on Inelastic State of Structures, Earthquake Spectra 23 (2007) 547–569.

[12] M. Motamedi, F. Nateghi, A Proposed Lateral Load Pattern Using Seismic Energy Distribution Along The Height Of Building, 14th World Conference on Earthquake Engineering, Beijing, China, October 12-17 (2008).

[13] M. Shahrouzi, A.A.Rahemi, Improved seismic design of structural frames by optimization of equivalent lateral load pattern, International Journal of Civil Engineering 12 (2014) 256–267.

[14] A. Kaveh, Advances in Metaheuristic Algorithms for Optimal Design of Structures, Springer International Publishing; 2017.

[15] Z.W. Geem, Novel Derivative of Harmony Search Algorithm for Discrete Design Variables, Applied Mathematics and Computation 199 (2008) 223–230.

[16] A. Kaveh, T. Bakhshpoori, A new metaheuristic for continuous structural optimization: water evaporation optimization, Structural and Multidisciplinary Optimization 54 (2016) 23–43.

[17] M. Shahrouzi, M. Pashaei, Stochastic Directional Search : an efficient heuristic for structural optimization of building frames, Scientia Iranica 20 (2013) 1124–1132.
[18] Z.W. Geem, Effects of Initial Memory and Identical Harmony in Global Optimization Using Harmony Search Algorithm, Applied Mathematics and Computation 218 (2012) 11337–11343.
[19] M. Shahrouzi, M. Aghabaglou, F. Rafiee, Observer-Teacher-Learner-Based Optimization: An enhanced meta-heuristic for structural sizing design, Structral Engineeirng and Mechanics 62 (2017) 537–550.
[20] M. Shahrouzi, Pseudo-random directional search: a new heuristic for optimization, International Journal of Optimization in Civil Engineering 1 (2011) 341–355.
[21] American Institute of Steel Construction, Allowable Stress Design and Plastic Design Specifications for Structural Steel Buildings, Chicago, Illinois, 1989.
[22] J. Holland, Adaptation in natural and artificial systems, an introductory analysis with application to biology, control and artificial intelligence, Ann Arbor, The University of Michigan Press, 1975.
[23] A. Kaveh, M. Shahrouzi, Direct index coding for discrete sizing optimization of structures by genetic algorithms, International Journal of Civil Engineering 3 (2005) 166–181.
[24] Pacific Earthquake Engineering Research Center, PEER Strong Motion Database, http://peer.berkeley.edu/.
[25] Federal Emergency Management Agency, FEMA 356: Prestandard and commentary for the seismic rehabilitation of buildings, Washington, US, 2000.